Thermochimica Acta 485 (2009) 1–13

Contents lists available at ScienceDirect

Thermochimica Acta

journal homepage: www.elsevier.com/locate/tca

Confined rapid thermolysis/FTIR/ToF studies of tetrazolium-based energetic ionic liquids

Arindrajit Chowdhury[a], Stefan T. Thynell[a,*], Ping Lin[b]

[a] Department of Mechanical and Nuclear Engineering, The Pennsylvania State University, University Park, PA 16802, USA
[b] Materials Research Institute, The Pennsylvania State University, University Park, PA 16802, USA

ARTICLE INFO

Article history:
Received 18 October 2008
Received in revised form
22 November 2008
Accepted 26 November 2008
Available online 13 December 2008

Keywords:
Ionic liquids
Thermal decomposition
FTIR spectroscopy
ToF mass spectrometry

ABSTRACT

The initiation of decomposition of several energetic ionic liquids (EILs) was studied by confined rapid thermolysis. Rapidscan FTIR spectroscopy and time-of-flight mass spectrometry were utilized to identify the products evolved from sub-milligram quantities subjected to heating rates of about 2000 K/s. The compounds studied were 2-amino-4,5-dimethyl-tetrazolium iodide (2AdMTZI), 2-amino-4,5-dimethyl-tetrazolium nitrate (2AdMTZN), 1-amino-4,5-dimethyl-tetrazolium iodide (1AdMTZI), and 1-amino-4,5-dimethyl-tetrazolium nitrate (1AdMTZN). Decomposition studies involving the 2AdMTZ salts were carried out around 300 °C. The major decomposition pathway involves a nucleophilic transfer to the anion leading to the formation of methyl iodide and methyl nitrate, from 2AdMTZI and 2AdMTZN, respectively. Methyl iodide ($m/z = 142$) was detected both in the ToFMS and FTIR spectra. Methyl nitrate ($m/z = 77$) was visible in the FTIR spectra. The resultant nitrogen-rich amino-methyl-tetrazole ($m/z = 99$) was found to decompose to form primarily molecular nitrogen and methyl isocyanide. Unlike the 2AdMTZ salts, the 1AdMTZ salts were found to initiate decomposition at temperatures lower by at least 50 °C. Decomposition was found to proceed through three major pathways—formation of the corresponding methylated anion and 1-amino-5-methyl-tetrazole, formation of ammonia by the amino group, and expulsion of nitrogen from the tetrazole cation itself. 1-Amino-5-methyl tetrazole was found to rapidly decompose to form mainly ammonia and nitrogen. The ammonia formed in the condensed phase during the decomposition of 1AdMTZN was reduced by methyl nitrate, to form smaller molecular weight species, such as N_2O, H_2O, NO_2, NO, CO_2, and others.

1. Introduction

Recent interest in ionic liquids, a unique class of salts with melting points below 100 °C, has been sparked due to their broad range of interesting properties [1–8]. The exceptional chemical and thermodynamic stability of these compounds, coupled with their low vapor pressures and low melting points have put them forth as potential replacements of many noxious organic solvents used in the chemical industry [9,10]. Also their easy recoverability after usage has made them popular as "green solvents". However, attention has recently been drawn to heterocyclic ionic liquids with nitrogen-rich cations, such as imidazoles, triazoles and, tetrazoles, coupled with oxygen-rich anions such as nitrates, nitramides, and perchlorates, because of their high energy density. These compounds are easy to synthesize and their properties can be tailored to suit specific requirements by minor alterations in their molecular structure.

The higher nitrogen content of the heterocyclic tetrazole compounds has prompted numerous studies on the compounds themselves and their derivatives. Experimental and numerical studies have been conducted on the thermal decomposition and combustion of tetrazole [11–14], amino-tetrazoles [15–18], nitramino-tetrazoles [19,20], nitro-tetrazoles [21–23], and even polymeric forms of tetrazoles [24,25]. Ab initio calculations on decomposition of substituted tetrazoles [26,27] indicate that ring-opening is initialized by N–N bond cleavage, instead of C–N bond scission.

The high heats of formation of nitrate, dinitramide, azide, and perchlorate salts of substituted tetrazoles, and production of high quantities of dinitrogen during decomposition has generated considerable interest in them as gas generators, propellants and explosives. However, limited knowledge is available in the literature on these energetic salts of tetrazoles. Shreeve and coworkers [28] synthesized nitrate and perchlorate salts of 2,4,5-trimethyltetrazolium and 4,5-dimethyl-1-aminotetrazolium cations. As observed with the triazole salts, the perchlorate salts were thermally more stable than the nitrate salts. Replacing a methyl group with an amino group lowers the onset of decomposition for both salts. Similar salts

* Corresponding author. Tel.: +1 814 863 0977; fax: +1 814 863 4848.
E-mail address: Thynell@psu.edu (S.T. Thynell).

0040-6031/$ – see front matter © 2008 Elsevier B.V. All rights reserved.
doi:10.1016/j.tca.2008.11.018

of 2-amino-4,5-dimethyltetrazolium cations [29] showed analogous decomposition trends.

Weigand and coworkers [30] prepared 1,5-diaminotetrazolium nitrate and perchlorate, and 1,5-diamino-4-methyl-tetrazolium nitrate, dinitramide, and azide salts. The salts were characterized by vibrational and NMR spectroscopy, mass spectrometry, X-ray crystallography and elemental analysis. The azide salt was found to be the least thermally stable, and provided the maximum molar enthalpy of formation. 1,5-Diaminotetrazolium perchlorate was also synthesized and studied by Drake et al. [31]. Diaminotetrazolium nitrate exhibited detonation velocities and pressures comparable to high explosives, such as HMX, RDX or PETN [32].

The slow thermal decomposition characteristics of derivatives of 1,5-diaminotetrazole were examined using thermogravimetric analysis and differential scanning calorimetry [33]. The gaseous products were identified by IR spectroscopy and mass spectrometry. Decomposition of the 1,5-diamino-4-methyl-1*H*-tetrazolium nitrate involved methyl group transfer to form $MeONO_2$, rather than proton transfer to form HNO_3. At heating rates of 10 °C/min, this ionic liquid began to decompose at 181 °C, and showed a peak heat release rate at 200 °C. The resultant 1,5-diaminotetrazole (DAT) readily produced nitrogen and an unstable nitrene, which subsequently produced ammonia and HCN. The azide salt decomposed through deprotonation to form 1-amino-4-methyl-5-imino-tetrazole and the corresponding acid HN_3. The decomposition temperatures were high enough to cause ring fracture of the tetrazole formed during the initiation step and led to the formation of smaller fragments, including methyl azide and aminocyanamide. The dinitramide salt also followed a similar deprotonation reaction to form 1-amino-4-methyl-5-imino-tetrazole and $HN(NO_2)_2$. $HN(NO_2)_2$ decomposes to N_2O and HNO_3, and HNO_3 promptly reacts with 1-amino-4-methyl-5-imino-tetrazole producing its nitrate salt, which decomposes in a manner discussed earlier.

Flash pyrolysis of 5-amino-1*H*-tetrazolium halides (chloride, bromide and iodide) was carried out by Brill and Ramanathan [15], and the products were identified by FTIR spectroscopy under temperatures ranging from 350 to 450 °C. The products indicated the presence of two different reaction pathways, the first being the dissociation of the salts to form molecular nitrogen. The remaining species decomposed spontaneously to form mainly HCN and the corresponding protonated anion (HCl, HBr, or HI). The second pathway involved deprotonation of the ring hydrogen and subsequent dissociation of 5-amino-tetrazole (5ATZ) into HN_3 and NH_2CN. The first channel of reaction is favored over the second in the order of $I^- > Br^- > Cl^-$, which is the same order as the basicities of these anions. The burning rates of the salts were found to be dependent on the extent of decomposition of 5ATZ molecule, rather than that of the $5ATZH^+$ ion.

In another pertinent work, Brill and coworkers [34] studied the different decomposition pathways occurring due to the presence of an amino group on the ring carbon (5-amino-tetrazole, 5ATZ) instead of a ring nitrogen (1-amino-tetrazole, 1ATZ). Rapid thermolysis of 1ATZ above 200 °C proceeded with the expulsion of HCN and N_2 from the ring leaving N_2H_2 to produce NH_3 and N_2. But the shift of the amino group prompts the scission of two weak ring N–N bonds to form HN_3 and NH_2CN as the principal products. As the temperatures were increased, NH_2CN trimerized to form the cyclic azine, melamine. The decomposition of two other compounds, 1,5-diamino-tetrazole and 2,5-diamino-tetrazole occurred through competitive reaction pathways, the first yielded HCN, whereas the second produced NH_2CN as the primary product. Both channels produced N_2 and NH_3 as the common species.

The concluded discussion illustrates that decomposition pathways of tetrazolium salts under high heating rates are not readily available in the literature. The aim of the current work is to identify the mechanism determining the initiation of decomposition of energetic tetrazolium salts under high temperatures and heating rates. The synergistic diagnostic tools, Fourier transform infrared (FTIR) spectroscopy and time-of-flight (ToF) mass spectrometry (MS), have been utilized to afford better probabilities of identifying the decomposition products and thus, accurately determining the reaction pathways. The energetic salts of primary interest are 1AdMTZN and 2AdMTZN. Since the complexity of the secondary reactions is considerably higher for the oxygen-rich anions, the relatively simple iodides 1AdMTZI and 2AdMTZI have been studied initially. The molecular structures of the molecules are shown in Fig. 1.

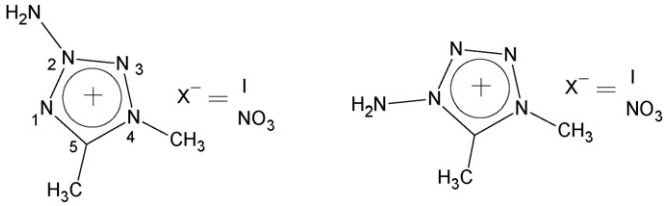

Fig. 1. Structures of 2-amino-4,5-dimethyl-tetrazolium X (X = iodide and nitrate), and 1-amino-4,5-dimethyl-tetrazolium X (X = iodide and nitrate).

2. Experimental approach

The experimental technique utilized to study the rapid thermal decomposition of the energetic materials is known as confined rapid thermolysis (CRT). The method involves rapidly heating a small quantity, typically 0.5 mg of a solid or 0.5 μL of a liquid, of the sample in between two heated surfaces maintained under isothermal conditions, in a constant pressure chamber purged by an inert gas. The decomposition products are quenched by a cool inert atmosphere as they evolve into the gas phase. This allows the decomposition processes occurring in the condensed phase to gain precedence over the gas-phase reactions. The heated surfaces are achieved by a stationary top heater and a mobile bottom heater, both of which are fitted with a cartridge heater, while temperature control is maintained by PID controllers. The use of a small sample volume enclosed in a confined space, roughly 300 μm in height, enables heating rates in the range of 2000 K/s. Two synergistic diagnostic tools, a Fourier transform infrared spectrometer and a time-of-flight mass spectrometer are used to study the temporal evolution of the gases from the condensed phase. Detailed discussion of the experimental setup and the data reduction techniques used to extract mole-fractions of individual species from the FTIR spectra have been discussed is earlier works [35–37].

A typical experiment consists of placing a small amount of the sample on a sample holder, which is brought in contact with the top heater by the bottom heater using a pneumatic piston cylinder mechanism. The gaseous products released from the condensed phase reactions are detected by the modulated beam from a Bruker IFS 66/S FTIR spectrometer in the rapid scanning mode, scanning at 2 cm^{-1} and with a temporal resolution of 50 ms. The species concentrations of various species, such as H_2O, N_2O, NO_2, NO, NH_3, CO_2, CO, MeOH, HCN, and HNO_3 are extracted by a non-linear, least-squares method by comparison with theoretical transmittance. The radiative properties, such as partition function, halfwidth of spectral lines, and its temperature exponent, are determined from the HITRAN data base [38]. N_2 was generated by these compounds, but it is not IR active. The gaseous species are also sampled by a ToFMS system, equipped with a 1 m flight tube and a 44 mm microchannel plate detector, via a 100 μm orifice plate. The molecular beam entering the third stage, maintained at 10^{-7} Torr, is ionized by electron impact ionization set at 70 eV. The high ionization levels result

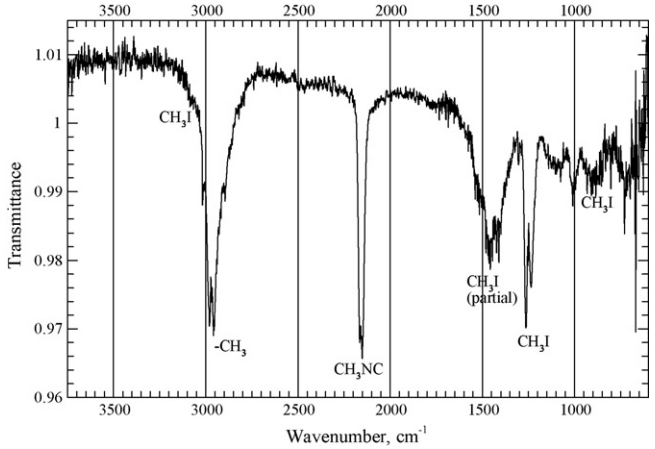

Fig. 2. FTIR spectrum of species from rapid thermolysis of 2AdMTZI at 320 °C and 1 atm N_2.

in severe fragmentation of the larger molecules, but this drawback is circumvented by the ability to compare with existing mass spectral and related data bases [39]. Individual mass spectra are acquired at 1000 Hz, and time-to-mass scaling is performed using the expressions $m = a(t - t_0)^2$, where the two constants for each mass spectrum are obtained from known positions of helium and argon.

3. Computational approach

The predicted reaction enthalpies and free energies were calculated using the Gaussian 03 suite of programs [40]. All geometrical structures were optimized using Density Functional Theory (DFT) with the B3LYP exchange correlation functional and 6-31++G** basis set, with the exception of iodine, for which 6-311G* [41], with extra diffuse functions [42], was used. Vibrational frequencies were calculated to confirm identification of the local minima and obtain thermodynamic properties. Enthalpies and free energies were calculated at 298 K and 1 atm pressure. In this study, calculations were carried out to identify the possible initiation steps during the decomposition of the energetic ionic compounds. A detailed study of the extensive set of secondary reactions as well as estimation of kinetic rate parameters using ab initio methods is the subject of future publications.

4. Results and discussion

4.1. Thermal decomposition pathways of 2AdMTZI

2AdMTZI is a dark brown crystalline solid under standard conditions, with a melting point of 124 °C [29]. The sample was dried in a vacuum chamber (40 mTorr) for 24 h and prepared for thermolysis. Approximately 0.5 mg of the sample was found to rapidly decompose above temperatures of 250 °C, leaving a small amount of spotted black residue on the aluminum foil. Thermolysis studies were carried out at temperatures around 300 °C. Fig. 2 shows the gaseous products from the decomposition of 2AdMTZI under 320 °C and an inert atmosphere of N_2. The vibrational frequencies of the experimentally observed species are listed in Table 1.

The major product identifiable from the FTIR spectrum is methyl iodide (CH_3I), with a strong stretch at 1252 cm^{-1}, and several other rovibrational bands. Lack of the $-NH_2$ stretches near 3450 cm^{-1} and the C–N stretch at 2260 cm^{-1} precluded the presence of cyanamide (NH_2CN) among the gaseous products. The rotational lines of the protonated anion, HI were not detected. The band near 2160 cm^{-1} is indicative of an azide N≡N stretch or an isocyanide

Table 1
Vibrational frequencies of experimentally observed gaseous products.

Description	Frequency (cm^{-1})
H_2O	3657 (s), 1595 (s)
HCN	3311 (s), 2097 (w), 712 (vs)
NH_3	3336 (m), 1626 (s), 968 (vs), 933 (vs)
CH_3I	3060 (m), 2970 (m), 2860 (m), 1435 (m), 1252 (s), 882 (m)
CH_3NC	3014 (s), 2966 (m), 2166 (m), 1466 (s)
$MeONO_2$	2959 (m), 2917 (m), 1678 (vs), 1661 (vs), 1442 (m), 1296 (s), 1278 (s), 1017 (s), 855 (s)
$MeNO_2$	2974 (w), 1584 (vs), 1438 (m), 1397 (s), 1378 (s), 1119 (w), 1099 (w), 918 (w), 657 (m)
MeONO	3016 (m), 2990 (m), 2950 (m), 1679 (vs), 1620 (vs), 1444 (m), 1046 (s), 991 (s), 812 (vs)
CO_2	3716 (w), 3609 (w), 2326 (vs), 741 (m), 667 (vs)
N_2O	2457 (vs), 2217 (vs), 1302 (vs), 1275 (vs)
NO	1876 (vs)
NO_2	2910 (m), 1621 (vs), 648 (w)
CH_3OH	3681 (m), 3000 (m), 2960 (s), 2844 (s), 1477 (m), 1345 (s), 1033 (vs)
CH_4	3019 (vs), 1306 (s)

N≡C stretch. Though an azide is a possible product during decomposition of tetrazoles, the azide N≡N stretch is accompanied by another prominent N–N stretch around 1150 cm^{-1}, thus negating its presence. Thus, the band was attributed to methyl isocyanide (CH_3NC) [39,43]. However, as seen in Fig. 3, at temperatures lower than 320 °C, the N≡C stretch was not visible, and further insights into its absence would be provided by the mass spectra. Also prominent was the absence of the inversion doublet of NH_3 (968 and 933 cm^{-1}), HCN (712 cm^{-1}), and CH_3CN (2267 cm^{-1}), all of which are probable species during degradation of the tetrazole ring with an amino group. N_2, which is a common product during the decomposition of tetrazole compounds, could not be detected due to its IR-inactivity. Based on the results of Figs. 2 and 3, the initiation of decomposition occurs most likely by the transfer of a methyl group from the cation to form CH_3I and the corresponding aminomethyl-tetrazole. Proton transfer does not occur directly to form HI.

To assist in the identification of species evolving during the decomposition of 2AdMTZI, Figs. 4 and 5 show the results from the thermolysis of 2AdMTZI under an inert atmosphere of Ar and He, acquired at 320 °C and 1 atm. Ar, He and residual air, under an ionization potential of 70 eV at 1000 Hz. In order to provide better signal-to-noise ratios in the mass spectra, 10 consecutive spectra were averaged. The standard deviation at any intensity due to this procedure was found to be below the acceptable limit of 5 units. Although the mass spectrum in Figs. 4 and 5, split in order to provide clarity, appears at a first glance as quite complicated due to

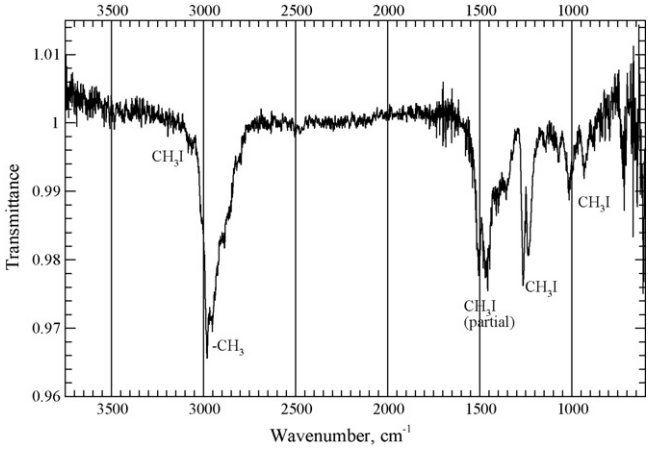

Fig. 3. FTIR spectrum of species from rapid thermolysis of 2AdMTZI at 300 °C and 1 atm N_2.

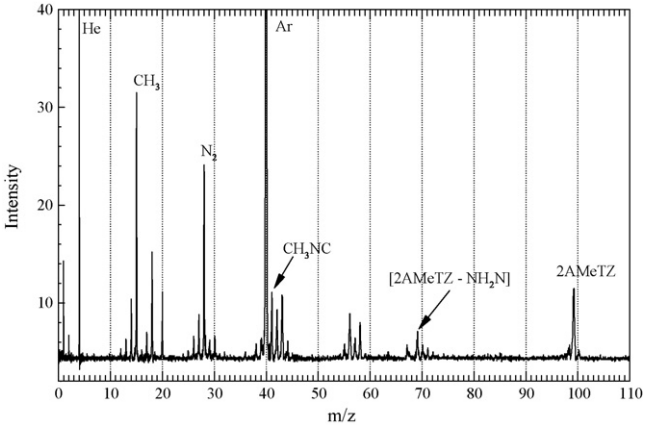

Fig. 4. Mass spectrum (m/z = 0–110) from rapid thermolysis of 2AdMTZI at 320 °C and 1 atm Ar, He and residual air extracted at 0.10 s (average of 10 spectra).

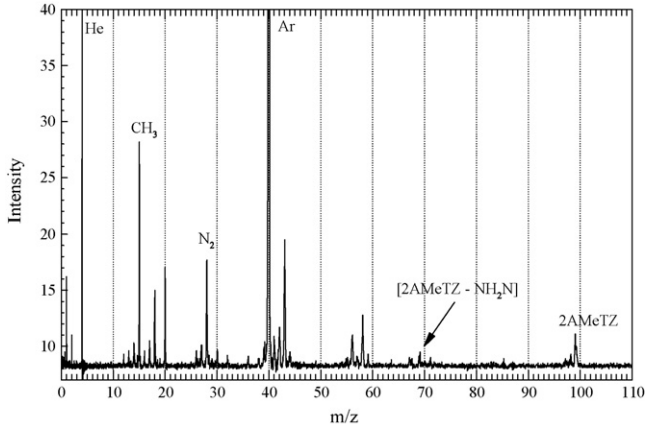

Fig. 6. Mass spectrum (m/z = 0–110) from rapid thermolysis of 2AdMTZI at 300 °C and 1 atm Ar, He and residual air extracted at 0.10 s (average of 10 spectra).

the fact that a high ionization potential is used, it facilitates comparison with available mass spectral data bases for a wide range of chemical compounds.

The peak at m/z = 142 in Fig. 5 attests the formation of CH_3I, which primarily accounts for the fragmented charged ion, CH_3^+ at m/z = 15. A strong peak at m/z = 99 is observed in Fig. 4, which can be formed by a methyl and an amino group attached to the tetrazole ring, thus corroborating the hypothesis derived from the FTIR spectrum that the amino group was indeed intact during the initiation reaction. N_2 was produced in abundant quantities. The CH_3NC observed in the FTIR spectra was confirmed by the peak at m/z = 41. However, as discussed previously, the relative intensity of this peak was smaller compared to the peak at m/z = 43 at lower temperatures, as shown by the mass spectra obtained at 300 °C in Figs. 6 and 7, coinciding with the disappearance of CH_3NC from the FTIR spectra. The appearance of peaks at m/z = 71, 69, 58, 56, 43, and 42 suggest the ring is fractured, both by the high ionization potentials used and the temperatures to which the amino-methyl-tetrazole was subjected. Detailed discussions of the possible fragmentation pathways of di-substituted tetrazoles are well-documented by Forkey and Carpenter [44]. The resultant amino-methyl-tetrazole dimerizes to a limited extent to form a di-tetrazole detected at m/z = 198.

The availability of the ToFMS data facilitates the determination of the decomposition pathways of 2AdMTZI. As discussed earlier, the nucleophilic transfer involves the formation of CH_3I and the corresponding amino-methyl-tetrazole. Since in general the bond dissociation energies of ring-*exo* C–C bonds are greater than ring-*exo* N–C bonds, the methyl group attached to the N(4) atom was preferably extracted to form CH_3I and 5-methyl-tetrazol-2-amine (2A5MeTZ). The theoretical results obtained for determination of the initiation reactions for 2AdMTZI at B3LYP/6-31++G** level are listed in Table 2. Reactions 1 and 3 show that the abstraction of the methyl group attached to the ring nitrogen is favorable over the abstraction from the ring carbon. The other explanation behind the selection of this initial step is that the reverse of this reaction is the synthesis procedure for 2AdMTZI [29]. As depicted by reaction 2, the secondary pathway, involving deamination to form NH_2I and 1,5-dimethyl-tetrazole (dMeTZ), is also energetically spontaneous. However, the absence of NH_2I, both in the FTIR spectra and the ToFMS spectra, lead to the conclusion that the minute quantities generated in the condensed phase engage in further secondary reactions to form other products. Due to almost undetectable levels of HI among the decomposition spectra, proton transfer from a methyl or amino group as an initiation reaction has been neglected as part of the calculations. Also neglected was ring-nitrogen expulsion as an initiation pathway, owing to the absence of two consecutive N atoms free from substituent groups.

It is well-established that thermal decomposition of tetrazoles is achieved by ring opening through either N_2 and/or azide elimination [45–47]. But, 2,5-disubstituted tetrazoles rarely undergo decomposition through splitting off an azide, and instead decompose through a ring-nitrogen expulsion to form an intermediate nitrilimine [48]. Besides, the formation of the amino azide would

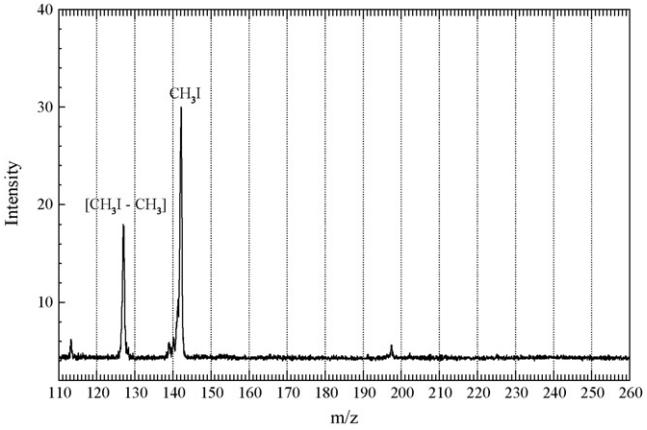

Fig. 5. Mass spectrum (m/z = 110–260) from rapid thermolysis of 2AdMTZI at 320 °C and 1 atm Ar, He and residual air extracted at 0.10 s (average of 10 spectra).

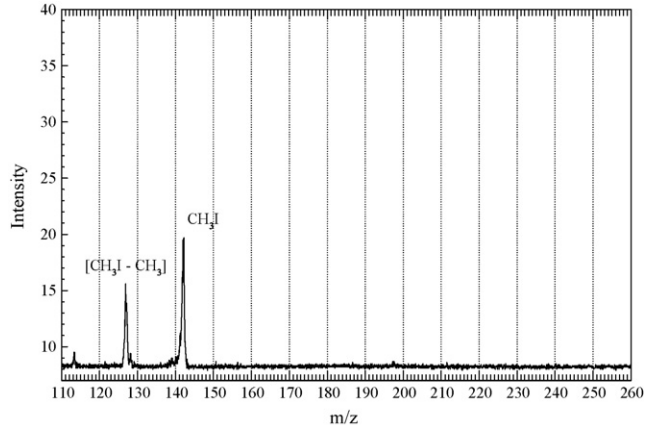

Fig. 7. Mass spectrum (m/z = 110–260) from rapid thermolysis of 2AdMTZI at 300 °C and 1 atm Ar, He and residual air extracted at 0.10 s (average of 10 spectra).

Table 2
Theoretical reaction enthalpies and free energies for 2AdMTZI at B3LYP/6-31++G** level.

Reactions	ΔH_R (kcal/mol)	ΔG_R (kcal/mol)
1 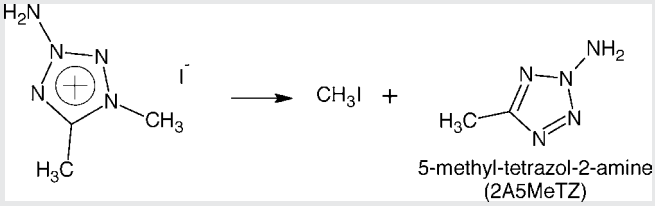	−9.96	−22.7
2 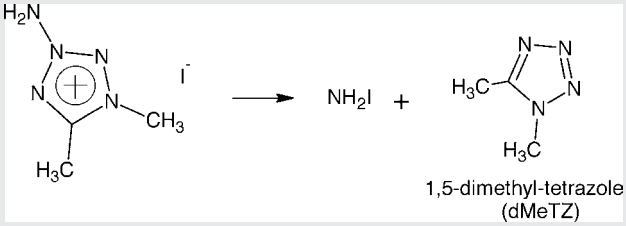	−12.9	−25.1
3 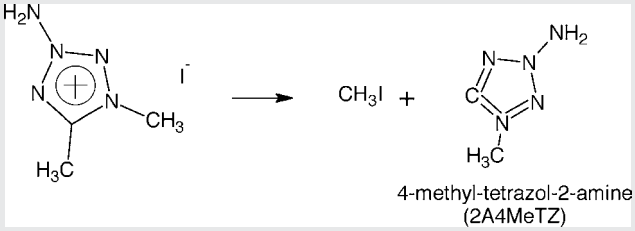	36.24	25.18

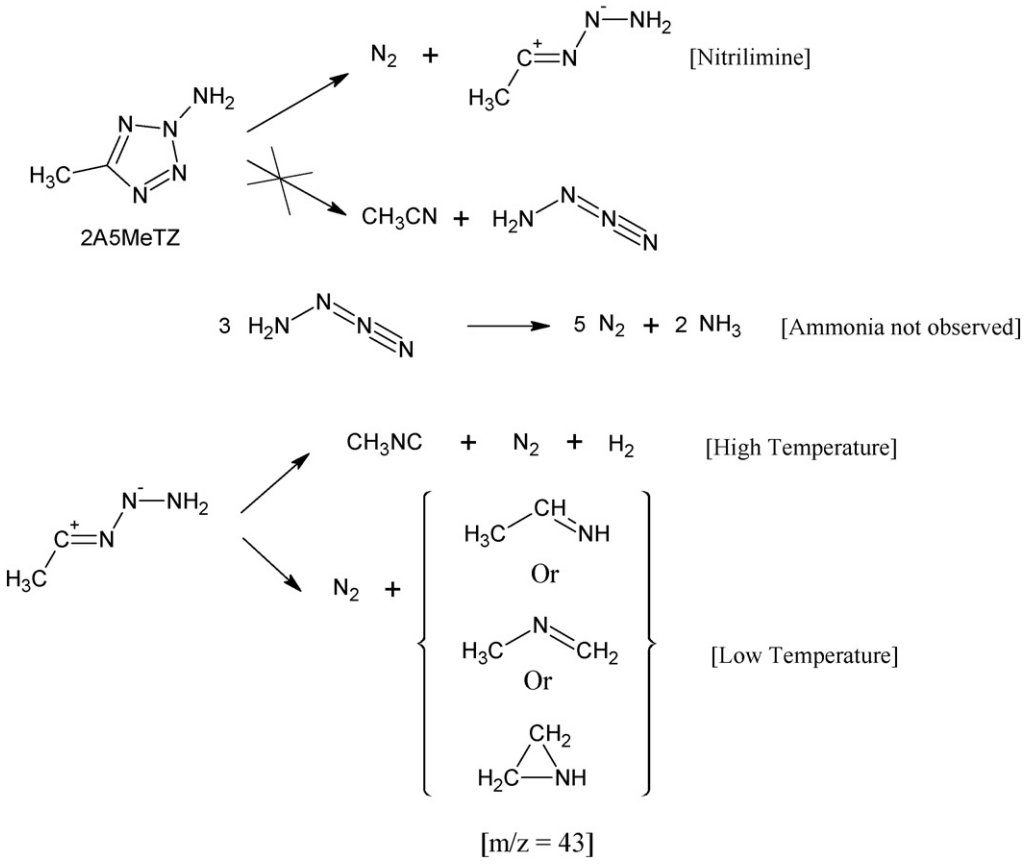

Pathway I. Considered secondary reaction pathways for 2AdMTZI.

entail the subsequent formation of ammonia, which is not observed in the FTIR spectra. At higher temperatures, the unstable nitrilimine stabilizes through the formation of methyl isocyanide and nitrogen. At lower temperatures, since the byproduct methyl isocyanide is absent and the peak at $m/z = 43$ dominates, it is possible that the nitrilimine forms *N*-methyl methanimine or an isomer through a second nitrogen elimination. If, for the sake of argument, formation of amino iodide (NH_2I) is indeed a major initiation step, and CH_3I is produced by a substitution reaction with the methyl group attached to the C(5) atom, forming 1-methyl-5-amino-tetrazole in the process, the FTIR spectra should have revealed NH_3, in accordance with the observations of Lesnikovich et al. [17]. If the substitution had occurred on the methyl group attached to the N(1) atom, forming 1-amino-5-methyl-tetrazole instead, large quantities of NH_3 should have been detected too, as will be elaborated in the following section (Pathway II).

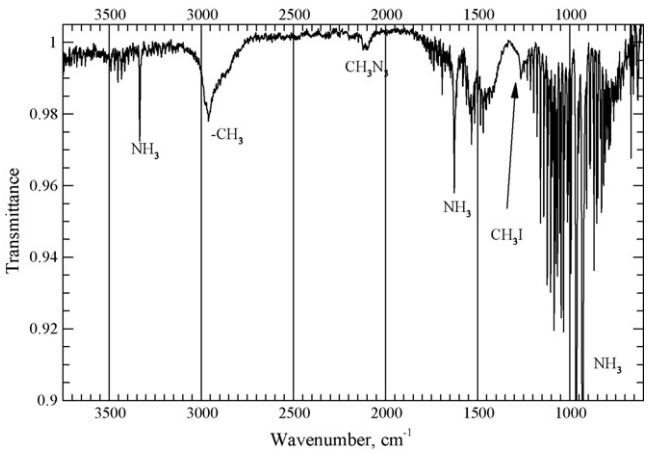

Fig. 8. FTIR spectrum of species from rapid thermolysis of 1AdMTZI at 250 °C and 1 atm N_2.

4.2. Thermal decomposition pathways of 1AdMTZI

1AdMTZI, an orange-colored crystalline solid under standard conditions, was thermally less stable than the 2-substituted tetrazolium salt. With a melting point similar to 2AdMTZI (121 °C),

Table 3
Theoretical reaction enthalpies and free energies for 1AdMTZI at B3LYP/6-31++G** level.

Reactions	ΔH_R (kcal/mol)	ΔG_R (kcal/mol)
1 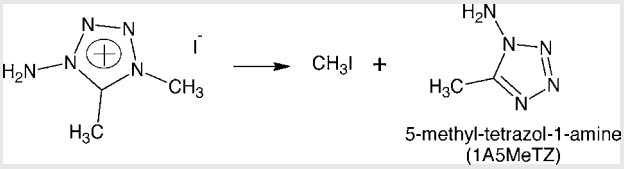	−4.13	−15.69
2 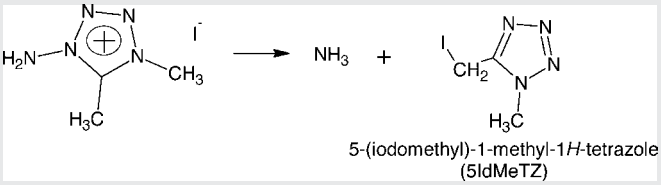	−17.73	−28.38
3 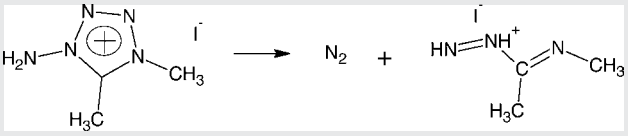	−29.55	−41.56
4 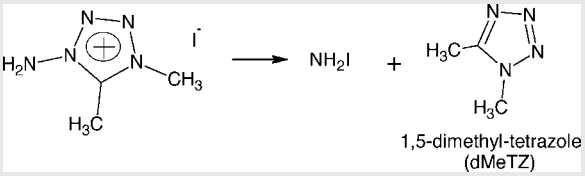	−7.95	−20.26
5 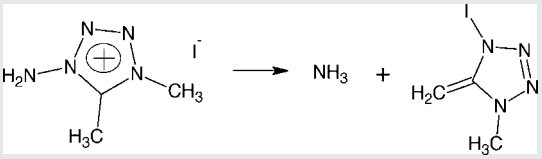	22.92	12.25
6 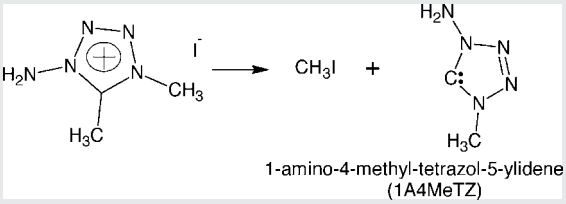	26.07	14.40

decomposition was initiated at temperatures 50 °C lower than 2AdMTZI. Thermolysis tests on the compound were typically conducted at 250 °C, leaving spotted black residues on the aluminum foil. Fig. 8 shows the species evolving from rapid thermolysis at 250 °C and 1 atm. As listed in Table 1, the principal product is ammonia, with its prominent rotational doublet and numerous rotational lines near 900 cm^{-1}. Also detected in the spectrum are vibrational bands from CH_3I. The strong absorption band near 3000 cm^{-1} is due to the $-CH_3$ group. Unlike 2AdMTZI, the important species CH_3NC was not present among the decomposition products. Also absent were HI, HCN, CH_3CN, NH_2CN, and HN_3. However, a weak band near 2104 cm^{-1} suggests the possible formation of CH_3N_3, whose rovibrational bands were listed by Fischer et al. [33]. The formation of CH_3I indicates an initiation reaction comparable to 2AdMTZI, proceeding through a methyl group transfer to the iodide anion, and leading to an amino-methyl-tetrazole, which reduces to smaller molecular weight species in subsequent steps. However, the prodigious amounts of NH_3 liberated leads to the possibility of the involvement of the amino group in the initiation reaction.

Results from the use of the ToFMS provide additional details on the rapid thermolysis behavior of 1AdMTZI. Figs. 9 and 10 show the results from an average of 10 mass spectra acquired at 1000 Hz. Hence the temporal resolution is 0.01 s. Careful observation of the spectra reveals that m/z = 142 (CH_3I), 15 (CH_3^+), 99 (an amino-methyl-tetrazole), and 17 (NH_3) are the major species. Also noticeable is the large peak of N_2 at m/z = 28. Smaller peaks at m/z = 113 and 198 (amino-methyl-tetrazole dimer) are also present, confirming similarities with 2AdMTZI. Smaller fragments from the tetrazole ring were identified at m/z = 69, 56, 41, 42, and 43. Their formation can be explained through familiar fragmentation pathways of 1,5-disubstituted tetrazoles [44]. The peak at m/z = 58 formed by the fragmentation of the amino-methyl-tetrazole detected in the mass spectra obtained during the thermolysis of 2AdMTZI was found to be absent in Fig. 9, thus confirming the presence of the amino group on a different N atom on the ring.

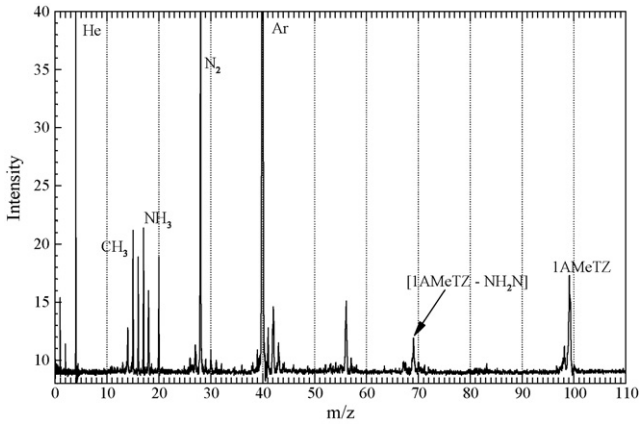

Fig. 9. Mass spectrum (m/z = 0–110) from rapid thermolysis of 1AdMTZI at 250 °C and 1 atm Ar, He and residual air extracted at 0.10 s (average of 10 spectra).

From the information revealed by the ToFMS and FTIR spectra, it is clear that the decomposition of 1AdMTZI proceeds through multiple reaction channels. The enthalpies and free energies of the possible initiation reactions calculated at B3LYP/6-31++G** are listed in Table 3. From the experimental results and theoretical calculations, it is clear that, as opposed to 2AdMTZI, the process of decomposition is not dominated solely by the methyl group transfer involving the cleavage of a ring-*exo* N–C bond, forming CH_3I and 5-methyl-tetrazol-1-amine (1A5MeTZ), as shown in reaction 1. Though the scission of the C–C bond to form CH_3I and 4-methyl-tetrazol-1-amine (1A4MeTZ) via reaction 6 was found to be energetically unfavorable and hence discarded, the copious quantity of ammonia and molecular nitrogen detected leads to

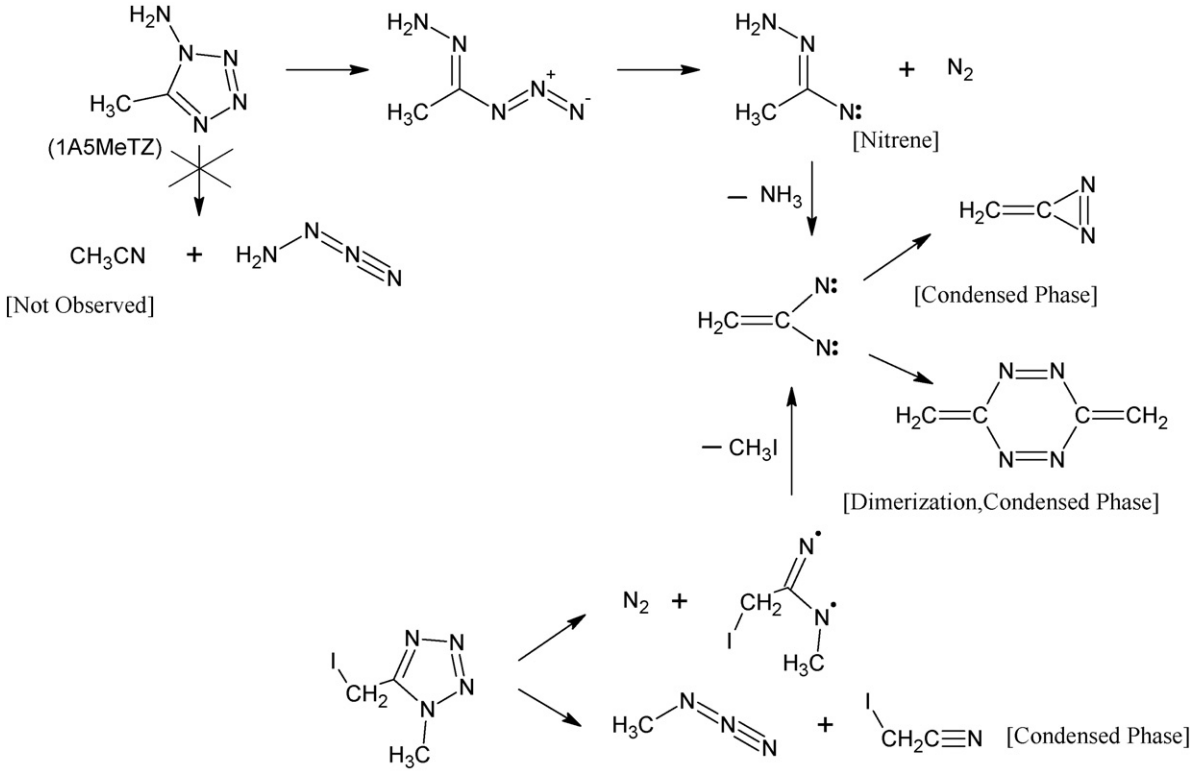

Pathway II. Considered secondary reaction pathways for 1AdMTZI.

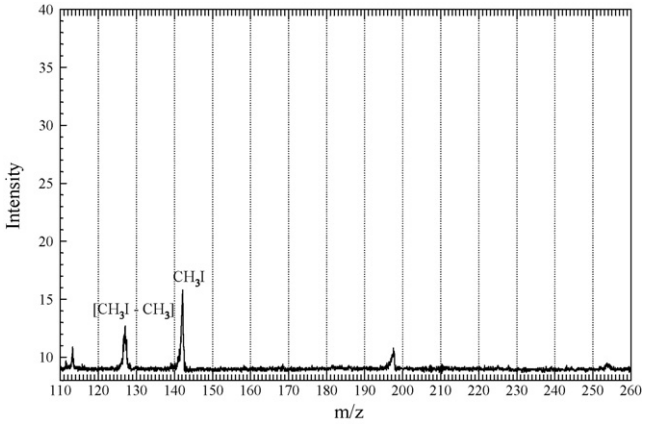

Fig. 10. Mass spectrum (m/z = 110–260) from rapid thermolysis of 1AdMTZI at 250 °C and 1 atm Ar, He and residual air extracted at 0.10 s (average of 10 spectra).

the possibility of two additional significant decomposition pathways. The first one, reaction 2, is initiated by the extraction of a hydrogen atom by the amino group from the neighboring methyl group to form NH_3 and 5-iodomethyl-tetrazol-1-amine (5IdMeTZ). The second one, reaction 3, is instigated by the removal of N_2 from the ring, and suggested by the decomposition characteristics of 5-amino-tetrazolium halides [15]. The remaining unstable species decomposes rapidly in the condensed phase to produce smaller products. The relative importance of the three pathways can be adjudged by further theoretical calculations to estimate their respective activation energies. As shown by reaction 4, the abstraction of the amino group to form NH_2I was also found to be plausible.

A complete enumeration of the numerous secondary reactions in the condensed phase is considerably challenging. However, the major secondary steps are shown in Pathway II. The di-substituted tetrazole, 1A5MeTZ rapidly decomposes under these conditions, aided by a ring N–N bond scission to form an isomeric azide [48,49], which releases nitrogen and a singlet nitrene. The nitrene proceeds to form NH_3 and other products, confined mainly to the condensed phase, in a manner similar to the decomposition of 1,5-diaminotetrazoles [17,33]. 5IdMeTZ decomposes either through the elimination of methyl azide and iodoacetonitrile, which remains in the condensed phase, or through the elimination of N_2 and CH_3I to form similar products during the decomposition of 1A5MeTZ.

4.3. Thermal decomposition pathways of 2AdMTZN

2AdMTZN is a white crystalline solid with a melting point of 94 °C, considerably lower than the corresponding iodide salt. The hygroscopic nature of the salt made it difficult to study the decomposition behavior of the compound. The sample was dried for 24 h under vacuum (40 mTorr) and then stored in a sealed container to avoid contamination by moisture. Small quantities of the sample were thermolysed at temperatures near 300 °C, with a sooty black residue left on the aluminum foil. Fig. 11 shows an FTIR spectrum of the gaseous products generated during the thermolysis of 2AdMTZN at 300 °C and 1 atm. Methyl nitrate (CH_3ONO_2), with several rovibrational bands from 1700 to 800 cm^{-1} was immediately discernable as the principal species. Also detected were H_2O, CO_2, and a small quantity of HCN. The common oxides of nitrogen, NO, N_2O, and NO_2 were surprisingly absent in Fig. 11. The double bands around 2260 and 2310 cm^{-1} were identified as a combination of methyl isocyanate (CH_3NCO) and CH_3CNO, respectively. Around 1750 cm^{-1}, a strong band due to a species containing a C=O bond was detected. Aldehydes and ketones normally show strong features in the range from 1700 to 1750 cm^{-1}. As found in the FTIR spectra of 2AdMTZI, CH_3NC was present with a band at 2160 cm^{-1}.

Fig. 12 shows a spectrum from the ToFMS acquired during the pyrolysis of 2AdMTZN at 300 °C and 1 atm Ar, He and residual air extracted 0.12 s after the two heaters came into contact. Although CH_3ONO_2 is absent from the mass spectrum at a cur-

Table 4
Theoretical reaction enthalpies and free energies for 2AdMTZN at B3LYP/6-31++G** level.

Reactions	ΔH_R (kcal/mol)	ΔG_R (kcal/mol)
1 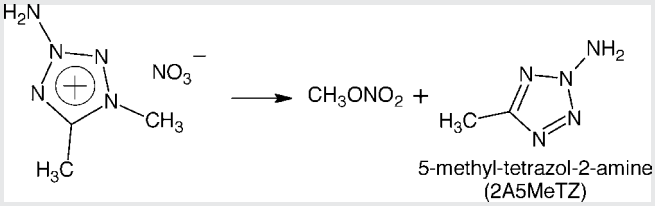	−3.42	−16.24
2 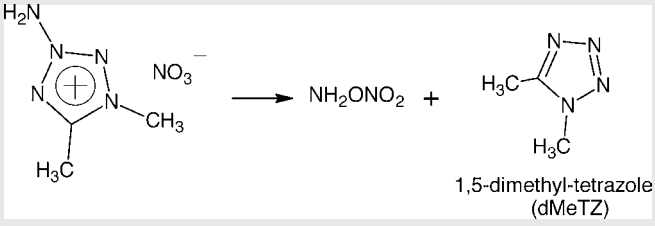	5.07	−6.68
3 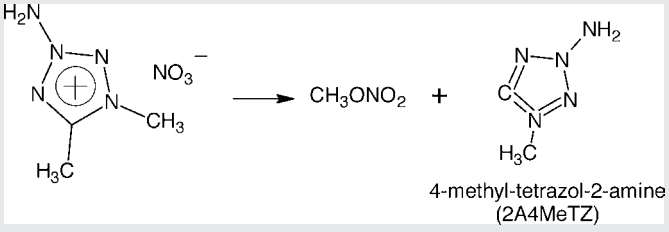	42.78	31.64

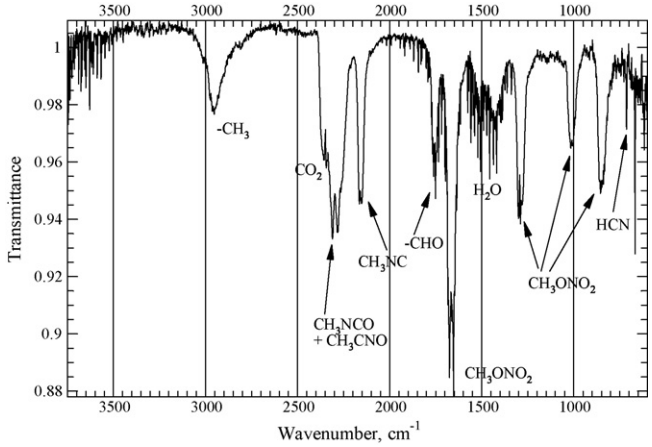

Fig. 11. FTIR spectrum of species from rapid thermolysis of 2AdMTZN at 300 °C and 1 atm N_2.

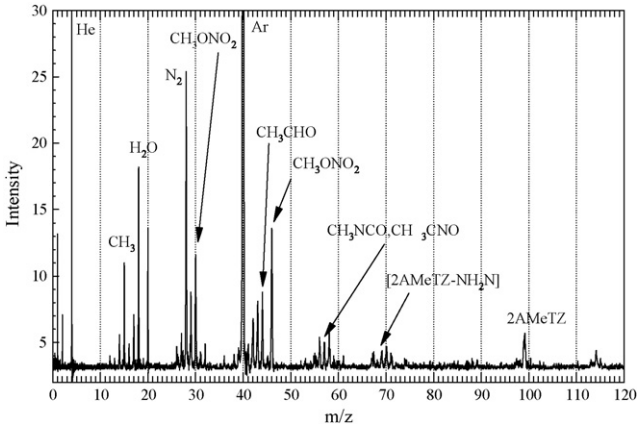

Fig. 12. Mass spectrum from rapid thermolysis of 2AdMTZN at 300 °C and 1 atm Ar, He and residual air extracted at 0.12 s (average of 10 spectra).

sory glance, its presence was confirmed by prominent peaks of CH_3^+ ($m/z = 15$), NO_2^+ ($m/z = 46$), and NO^+ ($m/z = 30$), corroborated by Fischer et al. during thermal decomposition of 1,5-diamino-4-methyl-tetrazolium nitrate [33]. The peak at $m/z = 99$ was confirmed as an amino-methyl-tetrazole, and after a brief study of the fragments, was identified as 2A5MeTZ. The smaller molecular-weight species of N_2 and H_2O were also present in Fig. 12. The larger peak at $m/z = 57$, in comparison to the mass spectra obtained during thermolysis of 2AdMTZI indicates that other species are present besides the fragments of 2A5MeTZ. The FTIR spectra confirm that these species are indeed CH_3NCO and CH_3CNO. The aldehyde present in the FTIR spectrum was recognized as acetaldehyde ($m/z = 44$) after deliberation.

The presence of the energetic nitrate anion and the complex structure of the tetrazole complicate the reactions leading to the decomposition of 2AdMTZN. However, the apparent abundance of CH_3ONO_2 and 2A5MeTZ indicates a similar initial reaction pathway as 2AdMTZI. Ab initio theoretical calculations at the B3LYP/6-31++G** level, shown in Table 4, corroborates that the major reaction channel remains unaltered from the one observed for 2AdMTZI. The affinity of the nitrate group for the methyl group over the amino group has also been established while studying decomposition behavior of 1,5-diamino-4-methyl-1*H*-tetrazolium nitrate [33].

The possible secondary reactions between the products formed are outlined in Pathway III. Majority of the generated CH_3ONO_2 in the condensed phase promptly escapes into the gas phase,

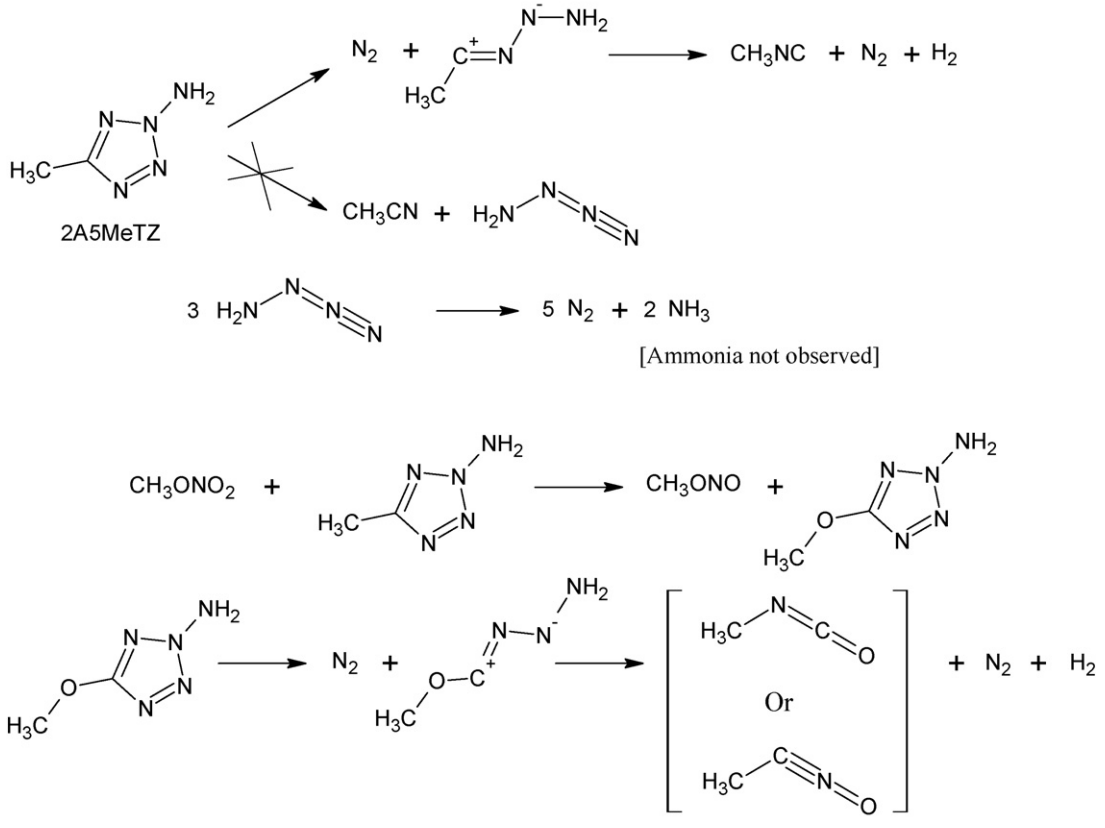

Pathway III. Considered secondary reaction pathways for 2AdMTZN.

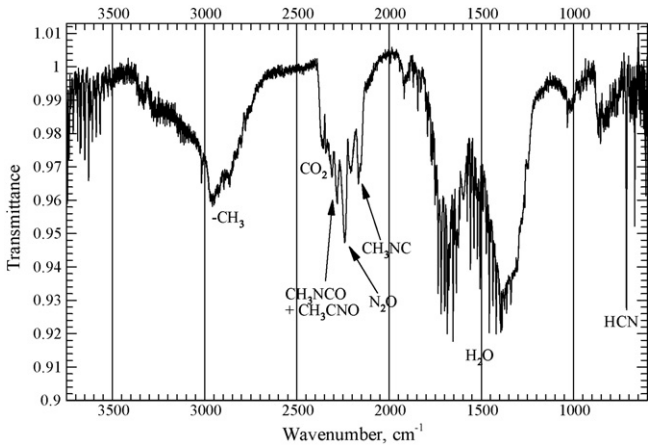

Fig. 13. FTIR spectrum of species from rapid thermolysis of 1AdMTZN at 250 °C and 1 atm N_2.

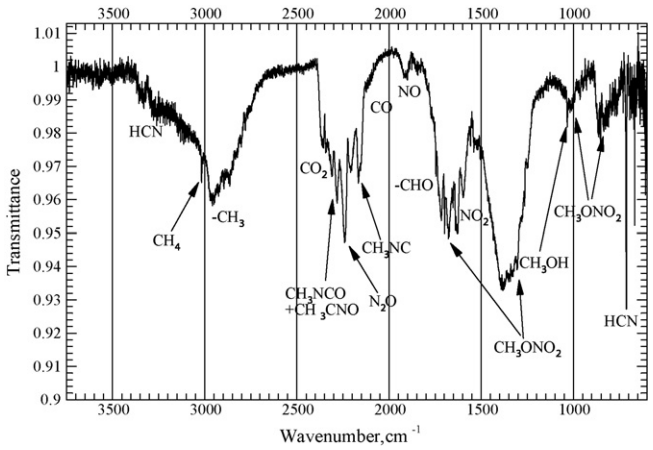

Fig. 14. FTIR spectrum of species from rapid thermolysis of 1AdMTZN at 250 °C and 1 atm N_2 (H_2O subtracted for clarity).

Table 5
Theoretical reaction enthalpies and free energies for 1AdMTZN at B3LYP/6-31++G** level.

Reactions	ΔH_R (kcal/mol)	ΔG_R (kcal/mol)
1 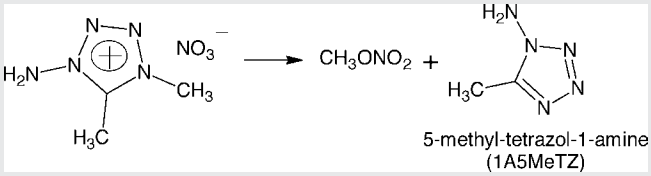	0.98	−10.68
2 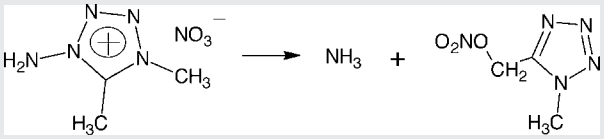	−15.86	−25.9
3 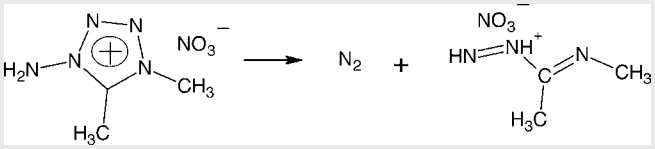	−16.24	−28.13
4 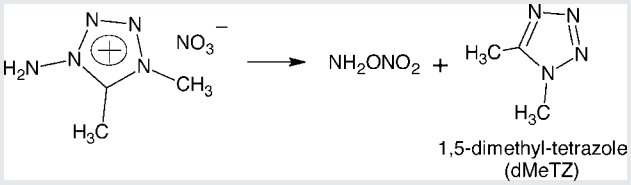	8.64	−3.31
5 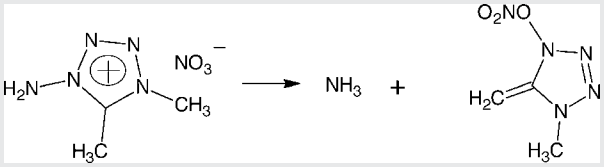	32.19	21.72
6 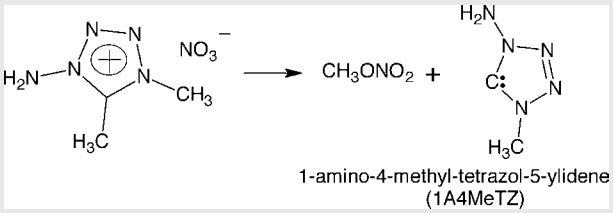	31.18	19.4

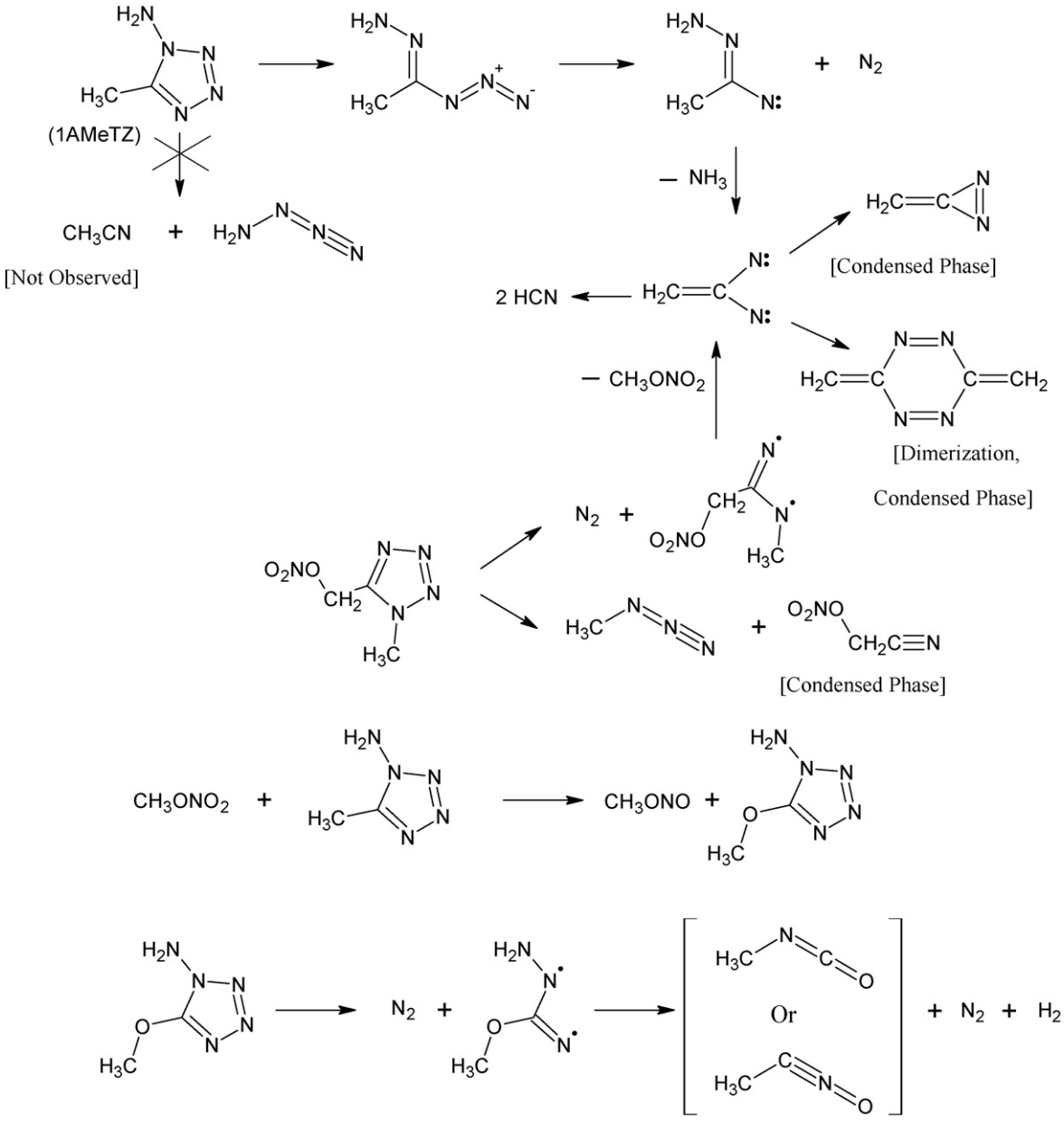

Pathway IV. Considered secondary reaction pathways for 1AdMTZN.

while the remaining amount reacts with 2A5MeTZ and its various intermediates. Subsequent reactions between CH_3ONO_2 and 2A5MeTZ replace the methyl group on 2A5MeTZ to form 2-amino-5-methoxy-2*H*-tetrazole, detected by a minor peak at $m/z = 115$ in Fig. 12, and methyl nitrite, CH_3ONO. Similar substitution reactions were observed during the thermolysis of di-alkyl-substituted imidazolium nitrates [36]. The methoxy tetrazole undergoes a decomposition process similar to 2A5MeTZ to form the species CH_3NCO and CH_3CNO through nitrogen elimination. Besides, CH_3ONO_2 and CH_3ONO partially decompose under the temperatures applied to form smaller molecules. Detailed discussions of these reactions, as well reactions involving partial decomposition of CH_3ONO_2 are beyond the scope of this paper. 2A5MeTZ itself also decomposes through previously described pathways.

4.4. Thermal decomposition pathways of 1AdMTZN

While the three tetrazolium salts studied prior to 1AdMTZN were all solids, this is a liquid under standard conditions with a melting temperature of −59 °C. Confined rapid thermolysis on approximately 0.5 μL of the sample was carried out at temperatures around 250 °C. Fig. 13 depicts an FTIR spectrum of species from rapid thermolysis of 1AdMTZN at 250 °C and 1 atm.

The spectrum is dominated by the rotational structures of H_2O, centered at 1595 cm^{-1}, making it difficult to ascertain the rovibrational bands present in the region 1200–2000 cm^{-1}. In order to determine the species present with water, the concentration of H_2O was calculated using a data reduction procedure and the amount of H_2O present was synthetically subtracted to yield the cleaner spectrum shown in Fig. 14. Consequently, the species that were identified are CH_3ONO_2, NO, NO_2, N_2O, CH_3CNO, and CH_3NCO. Also detected in smaller quantities were CO, CO_2, CH_4, and CH_3OH. Although not detected among the decomposition products of 1AdMTZI, HCN with its strong Q-branch at 712 cm^{-1}, was identified in Fig. 14. The large quantities of NH_3 found in the FTIR spectra of 1AdMTZI were oxidized by methyl nitrate formed during the initiation step. An aldehyde was identified by the prominent band near

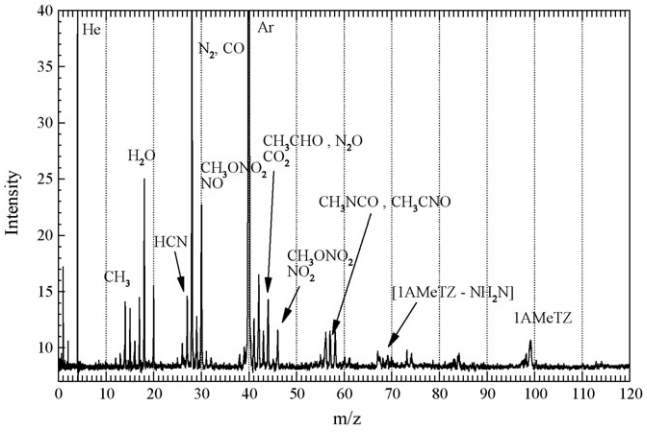

Fig. 15. Mass spectrum from rapid thermolysis of 1AdMTZN at 250 °C and 1 atm Ar, He and residual air extracted at 0.09 s (average of 10 spectra).

1750 cm^{-1}. Additionally, the N≡C stretch from the isonitrile, CH_3NC was found at 2160 cm^{-1}.

Fig. 15 shows a ToFMS spectrum from the thermolysis of 1AdMTZN, taken 0.09 s after initiation of heating at 250 °C and 1 atm Ar, He and residual air. Similar to 2AdMTZN, the decomposition products include CH_3ONO_2. Also present are 1A5MeTZ at m/z = 99, NO_2 at m/z = 46, N_2O and CO_2 at m/z = 44, NO at m/z = 30, CO and N_2 at m/z = 28, HCN at m/z = 27, and H_2O at m/z = 18. The peak at m/z = 57 corroborates the presence of CH_3NCO and CH_3CNO.

Based on the FTIR and ToFMS data, and the previous knowledge gained from studying the decomposition of 1AdMTZI, the primary reaction pathways and their associated free energy changes calculated at the B3LYP/6-31++G** level have been tabulated in Table 5. As expected, three major pathways—a nucleophilic transfer involving the methyl group attached to the ring nitrogen to form 1A5MeTZ and CH_3ONO_2 (reaction 1), ammonia formation by the amino group through a proton abstraction from the neighboring methyl group (reaction 2), as well as ring nitrogen elimination (reaction 3), were all found to be thermodynamically feasible processes. As found before in the case of 1AdMTZI, the formation of 1A4MeTZ was found to be unfavorable in reaction 6. A detailed description of the secondary reactions leading to the detected species portrayed in Figs. 13–15 has been given in Pathway IV. 1A5MeTZ dissociates with an N_2 ejection to form mainly ammonia. Unlike the decomposition of 2AdMTZN, where most of the generated CH_3ONO_2 desorbed into the gas phase, majority of the nitrate from 1AdMTZN oxidizes NH_3 to liberate a number of smaller molecular weight species, namely N_2O and H_2O, as well as CO, NO, CO_2, and NO_2. A portion of CH_3ONO_2 reacts through the formation of 1-amino-5-methoxy-1*H*-tetrazole to form CH_3NCO and CH_3CNO, forming CH_3ONO in the process. Besides these primary reactions, numerous other secondary reactions involving the intermediate nitrenes, CH_3ONO_2, and CH_3ONO also take place to form the smaller molecular weight gases.

5. Conclusions

Confined rapid thermolysis studies with FTIR spectroscopy and ToF mass spectrometry as the diagnostic tools were conducted on four tetrazolium-based compounds, 2AdMTZI, 2AdMTZN, 1AdMTZI, and 1AdMTZN. The relocation of the amino group from the N(2) position to the N(1) position lowered the thermal stability of the salts by 50 °C. While in case of 2AdMTZI and 2AdMTZN, the nucleophilic transfer primarily involved a methyl group, despite the presence of a more reactive amino substituent on the ring, in case of 1AdMTZI and 1AdMTZN, initiation reactions involved the methyl group extraction, hydrogen abstraction by the amino group, and ring nitrogen expulsion. The resultant amino-methyl-tetrazoles decomposed readily. 2A5MeTZ formed N_2 and CH_3NC as the principal products at higher temperatures, while 1A5MeTZ formed NH_3 and N_2. Methyl nitrate formed in the initial steps from the nitrate salts participated in a series of complex secondary reactions to form smaller species.

Acknowledgments

This material is based upon work supported by the U. S. Air Force Office of Scientific Research under Contract No. FA9550-07-1-0432, with Dr. Michael Berman serving as the program manager. The authors are grateful to Drs. J.M. Shreeve and Hong Xue of the University of Idaho for the preparation and shipment of the materials used in this study.

References

[1] A.A. Fannin, D.A. Floreani, L.A. King, J.S. Landers, B.J. Piersma, D.J. Stech, R.L. Vaughn, J.S. Wilkes, J.L. Williams, J. Phys. Chem. 88 (1984) 2614–2627.
[2] J.S. Wilkes, M.J. Zaworotko, J. Chem. Soc., Chem. Commun. (1992) 965–967.
[3] J.D. Holbrey, K.R. Seddon, Clean Prod. Process. 1 (4) (1999) 223–236.
[4] A.S. Larsen, J.D. Holbrey, F.S. Tham, C.A. Reed, J. Am. Chem. Soc. 122 (2000) 7265–7272.
[5] J.S. Wilkes, J.A. Levisky, R.A. Wilson, C.L. Hussey, Inorg. Chem. 21 (3) (1982) 1263–1264.
[6] J. Sun, M. Forsyth, D.R. MacFarlane, J. Phys. Chem. B 102 (44) (1998) 8858–8864.
[7] P. Bônhote, A.-P. Dias, N. Papageorgiou, K. Kalyanasundaram, M. Grätzel, Inorg. Chem. 35 (5) (1996) 1168–1178.
[8] J. Shah, J. Brennecke, E. Maginn, Green Chem. 4 (2002) 112–118.
[9] M.J. Earle, K.R. Seddon, Pure Appl. Chem. 72 (7) (2000) 1391–1398.
[10] T. Welton, Chem. Rev. 99 (1999) 2071–2083.
[11] S. Kawaguchi, M. Kumasaki, Y. Wada, M. Arai, M. Tamura, J. Jpn. Explosives Soc. 62 (2001) 16–22.
[12] V.P. Sinditskii, V.Y. Egorshev, V.V. Sherushkin, A.E. Fogelzang, V.I. Kolesov, Proceedings of the 29th International Annual Conference of ICT, Karlsruhe, Germany, 1998, pp. 171-1–171-114.
[13] A.E. Fogelzang, V.P. Sinditskii, V.Y. Egorshev, V.V. Sherushkin, Decomposition, Combustion, and Detonation Chemistry of Energetic Materials, MRS Symposium Proc. 418, Pittsburgh, PA, 1996, pp. 151–161.
[14] A.I. Lesnikovich, G.V. Printsev, O.A. Ivachkevich, V.A. Lutsko, K.K. Kovalenko, Fizika Gorenia i Vzryva [Detonation and Shock Waves] 24 (1988) 48–51.
[15] T.B. Brill, H. Ramanathan, Combust. Flame 122 (2000) 165–171.
[16] A.M. Helmy, W. Tong, 36th AIAA/ASME/SAE/ASEE Joint Propulsion Conference and Exhibit, Huntsville, AL, 2000, AIAA Paper 2000-3330.
[17] A.I. Lesnikovich, O.A. Ivashkevich, S.V. Levchik, A.I. Balabanovich, P.N. Gaponik, A.A. Kulak, Thermochim. Acta 388 (2002) 233–251.
[18] S.V. Levchik, A.I. Balabanovich, O.A. Ivashkevich, A.I. Lesnikovich, P.N. Gaponik, L. Costa, Thermochim. Acta 225 (1993) 53–65.
[19] A. Gao, A.L. Rheingold, T.B. Brill, Prop. Explosives Pyrotech. 16 (3) (1991) 97–104.
[20] B.C. Tappan, C.D. Incarvito, A.L. Rheingold, T.B. Brill, Thermochim. Acta 384 (2002) 113–120.
[21] R.J. Spear, Materials Research Labs., Melbourne (Australia), Technical Report Number MRL-R-780-PT-1, AR-002-165-PT-1.
[22] M.B. Talawar, A.P. Agrawal, M. Anniyappan, D.S. Wani, M.K. Bansode, G.M. Gore, J. Hazard. Mater. 137 (2) (2006) 1074–1078.
[23] J. Wang, J. Gu, A. Tian, Chem. Phys. Lett. 351 (5–6) (2002) 459–468.
[24] S.V. Levchik, A.I. Balabanovich, O.A. Ivashkevich, P.N. Gaponik, L. Costa, Polym. Degrad. Stabil. 47 (3) (1995) 333.
[25] S.V. Levchik, O.A. Ivashkevich, L. Costa, P.N. Gaponik, T.N. Andreeva, Polym. Degrad. Stabil. 46 (2) (1994) 225–234.
[26] Y.M. Ohno, M. Arai, M. Tamura, T. Matsunaga, J. Jpn. Explosives Soc. 60 (1999) 212–219.
[27] J. Wang, J. Gub, A. Tian, Chem. Phys. Lett. 351 (2002) 459–468.
[28] H. Xue, Y. Gao, B. Twamley, J.M. Shreeve, Chem. Mater. 17 (2005) 191–198.
[29] H. Xue, S.W. Arritt, B. Twamley, J.M. Shreeve, Inorg. Chem. 43 (2004) 7972–7977.
[30] J.C. Galvez-Ruiz, G. Holl, K. Karaghiosoff, T.M. Klapötke, K. Lohnwitz, P. Mayer, H. Noth, K. Polborn, C.J. Rohbogner, M. Suter, J.J. Weigand, Inorg. Chem. 44 (12) (2005) 4237–4253.
[31] G.W. Drake, T.W. Hawkins, J. Boatz, L. Hall, A. Vij, Prop. Explosives Pyrotech. 30 (2) (2005) 156–163.
[32] J. Geith, T.M. Klapötke, J. Weigand, G. Holl, Prop. Explosives Pyrotech. 29 (1) (2004) 3–8.
[33] G. Fischer, G. Holl, T.M. Klapötke, J.J. Weigand, Thermochim. Acta 437 (1–2) (2005) 168–178.
[34] A. Gao, Y. Oyumi, T.B. Brill, Combust. Flame 83 (1991) 345–352.
[35] E.S. Kim, H.S. Lee, C.F. Mallery, S.T. Thynell, Combust. Flame 110 (1997) 239–255.
[36] A. Chowdhury, S.T. Thynell, Thermochim. Acta 443 (2006) 164–177.
[37] C.F. Mallery, S.T. Thynell, Combust. Sci. Technol. 122 (1997) 113–129.

[38] L.S. Rothman, D. Jacquemart, A. Barbe, D. Chris Benner, M. Birk, L.R. Brown, M.R. Carleer, J.C. Chackerian, K. Chance, L.H. Coudert, V. Dana, V.M. Devi, J.M. Flaud, R.R. Gamache, A. Goldman, J.M. Hartmann, K.W. Jucks, A.G. Maki, J.Y. Mandin, S.T. Massie, J. Orphal, A. Perrin, C.P. Rinsland, M.A.H. Smith, J. Tennyson, R.N. Tolchenov, R.A. Toth, J. Vander Auwera, P. Varanasi, G. Wagner, J. Quant. Spectrosc. Radiat. Transfer 96 (2) (2005) 139–204.
[39] P.J. Linstrom, W.G. Mallard (Eds.), NIST Chemistry WebBook, NIST Standard Reference Database Number 69, National Institute of Standards and Technology, Gaithersburg MD, 20899, 2005.
[40] M.J. Frisch, G.W. Trucks, H.B. Schlegel, G.E. Scuseria, M.A. Robb, J.R. Cheeseman, J.A. Montgomery Jr., T. Vreven, K.N. Kudin, J.C. Burant, J.M. Millam, S.S. Iyengar, J. Tomasi, V. Barone, B. Mennucci, M. Cossi, G. Scalmani, N. Rega, G.A. Petersson, H. Nakatsuji, M. Hada, M. Ehara, K. Toyota, R. Fukuda, J. Hasegawa, M. Ishida, T. Nakajima, Y. Honda, O. Kitao, H. Nakai, M. Klene, X. Li, J.E. Knox, H.P. Hratchian, J.B. Cross, V. Bakken, C. Adamo, J. Jaramillo, R. Gomperts, R.E. Stratmann, O. Yazyev, A.J. Austin, R. Cammi, C. Pomelli, J.W. Ochterski, P.Y. Ayala, K. Morokuma, G.A. Voth, P. Salvador, J.J. Dannenberg, V.G. Zakrzewski, S. Dapprich, A.D. Daniels, M.C. Strain, O. Farkas, D.K. Malick, A.D. Rabuck, K. Raghavachari, J.B. Foresman, J.V. Ortiz, Q. Cui, A.G. Baboul, S. Clifford, J. Cioslowski, B.B. Stefanov, G. Liu, A. Liashenko, P. Piskorz, I. Komaromi, R.L. Martin, D.J. Fox, T. Keith, M.A. Al-Laham, C.Y. Peng, A. Nanayakkara, M. Challacombe, P.M.W. Gill, B. Johnson, W. Chen, M.W. Wong, C. Gonzalez, J.A. Pople, Gaussian 03, Revision C.02, Gaussian, Inc., Wallingford CT, 2004.
[41] M.N. Glukhovstev, A. Pross, M.P. McGrath, L. Radom, J. Chem. Phys. 103 (1995) 1878–1885.
[42] K.A. Peterson, B.C. Shepler, D. Figgen, H. Stoll, J. Phys. Chem. A 110 (2006) 13877–13883.
[43] M. Khilifi, P. Paillous, P. Bruston, F. Raulin, J.C. Guillemin, Icarus 124 (1996) 318–328.
[44] D.M. Forkey, W.R. Carpenter, Org. Mass Spectrom. 2 (1969) 433–445.
[45] S. Löbbecke, A. Pfeil, H.H. Krause, J. Sauer, U. Holland, Prop. Explosives Pyrotech. 24 (1999) 168–175.
[46] M. Seidl, Ph.D. Thesis, University of München, Germany, 1960.
[47] V.V. Nedelko, V.P. Roshchupkin, S.V. Kurmaz, T.S. Larikova, A.I. Lesnikovich, O.A. Ivashkevich, S.V. Levchik, E.E. Bolvanovich, P.N. Gaponik, Thermochim. Acta 179 (1991) 201.
[48] A.I. Lesnikovich, S.V. Levchik, A.I. Balabanovich, O.A. Ivachkevich, P.N. Gaponik, Thermochim. Acta 200 (1992) 427–441.
[49] P.A.S. Smith, J. Am. Chem. Soc. 76 (1954) 436.